

**Pyrene containing liquid crystalline asymmetric phthalocyanines and their composite materials with single-walled carbon nanotubes**

KAYA, Esra Nur, POLYAKOV, Maxim S., BASOVA, Tamara V., DURMUŞ, Mahmut and HASSAN, Aseel <<http://orcid.org/0000-0002-7891-8087>>

Available from Sheffield Hallam University Research Archive (SHURA) at:

<https://shura.shu.ac.uk/18578/>

---

This document is the Accepted Version [AM]

**Citation:**

KAYA, Esra Nur, POLYAKOV, Maxim S., BASOVA, Tamara V., DURMUŞ, Mahmut and HASSAN, Aseel (2018). Pyrene containing liquid crystalline asymmetric phthalocyanines and their composite materials with single-walled carbon nanotubes. *Journal of Porphyrins and Phthalocyanines*, 22 (1), 56-63. [Article]

---

**Copyright and re-use policy**

See <http://shura.shu.ac.uk/information.html>

# Pyrene Containing Liquid Crystalline Asymmetric Phthalocyanines and their Composite Materials with Single-Walled Carbon Nanotubes

Esra Nur Kaya<sup>a</sup>, Maxim S. Polyakov<sup>b</sup>, Tamara V. Basova<sup>\*b,c</sup>, Mahmut Durmuş<sup>a</sup>, Aseel Hassan<sup>d</sup>

<sup>a</sup>*Gebze Technical University, Department of Chemistry, Gebze, Kocaeli 41400, Turkey*

<sup>b</sup>*Nikolaev Institutes of Inorganic Chemistry SB RAS, Lavrentiev Pr. 3, Novosibirsk 630090, Russia*

<sup>c</sup>*Novosibirsk State University, Pirogova Str. 2, Novosibirsk 630090,*

<sup>d</sup>*Material and Engineering Research Institute, Sheffield Hallam University, Sheffield UK*

*Received date*

*Accepted date*

**ABSTRACT:** In the present work we have studied the dispersion of single-walled carbon nanotubes (SWCNTs) in liquid crystalline asymmetrically substituted phthalocyanines (MPc, where M=Cu, Co, and H<sub>2</sub>) bearing one pyrene and six polyoxy groups as side chains. The influence of SWCNT on the phase behavior of MPcs was investigated using X-ray diffraction XRD, polarized optical microscopy and differential scanning calorimetry. It was demonstrated that the incorporation of small amounts of SWCNT ( $\leq 1$  wt. %) does not alter the MPc mesophases. The structural features and the sensor response of MPc/SWCNT composite thin films to ammonia vapour (10-50 ppm) was studied and compared with those of the films of pure MPc derivatives.

**KEYWORDS:** Liquid crystals, Phthalocyanines, Composite materials, Carbon nanotubes, Sensors

\*Correspondence to: Dr. Tamara Basova, Nikolaev Institutes of Inorganic Chemistry SB RAS, Lavrentiev Pr. 3, Novosibirsk, Russia  
Tel.: +7 383 3308957; fax: +7 383 3309489; e-mail: basova@niic.nsc.ru.

## INTRODUCTION

Metal phthalocyanines and porphyrins coupled with different carbon nanomaterials are of great interest due to their ability to form long-lived charge separated states which makes them useful for application in photonics and solar energy harvesting [1-4]. A combination of such important properties of carbon nanomaterials as their electrical conductivity and large surface area together with the sensitivity and selectivity of phthalocyanines to different chemical analytes provides an effective use of hybrids of these materials as active layers of chemical sensors [5-6].

Among various metal phthalocyanines liquid crystalline (LC) phthalocyanines with long alkyl substituents play significant role as active layers in different electronic devices including chemical sensors [7-9]. On the one hand, LC phthalocyanines form films with controllable alignment and ordering and the efficient overlap of  $\pi$  electron orbitals of neighboring phthalocyanine macrocycles in stacks provides anisotropic electronic transport channels along columnar axis [10-11].

Hybrids and composites of carbon nanomaterials with phthalocyanines are known to be obtained using three different ways, namely by covalent and noncovalent functionalization [12-14] of CNT or graphene with phthalocyanine derivatives and by preparation of blends containing various ratios of these two components [15]. In the literature, hybrids are referred to as materials where the main component is a carbon nanomaterial (carbon nanotubes, graphene etc.), while phthalocyanines are attached to them *via*  $\pi$ - $\pi$  interaction or covalent bondings. Composites are said to be materials consisting of a phthalocyanine derivative as the main matrix in which a small amount of a carbon nanomaterial is dispersed. Hybrids of carbon nanotubes and graphene with covalently and noncovalently attached metal phthalocyanine derivatives have been studied in the literature from different points of view [1, 13, 16, 17]. The use of hybrids of these materials for the development of chemiresistive sensors has been extensively studied in recent years [18-23]. In our recent publications, we studied sensor properties of hybrids of single walled carbon nanotubes and reduced graphene oxide with symmetrically polyoxyethylene octasubstituted MPc (M=H<sub>2</sub>, Zn, Cu, Co) and similar asymmetrically substituted ZnPc [5, 23]. Those hybrids were obtained by covalent and noncovalent attachment of the phthalocyanines to the carbon nanomaterials. At the same time, the studies of composite materials obtained by dispersion of small amounts of carbon nanomaterials in the MPc matrix, including distribution and alignment of CNTs in the matrix of liquid crystalline phthalocyanines are rather scarce and were published only in a few papers using only one ZnPc derivative [15]. A blend of ZnPc bearing 16 long alkane moieties with fullerene C<sub>60</sub> was produced to promote self-organization on a substrate surface [24]. In our recent work we studied the distribution of SWCNT in the ordered matrix of polyoxyethylene symmetrically substituted (B4 type) and pyrene containing asymmetrically substituted (AB3 type) zinc(II) phthalocyanine derivatives [15]. Pyrene groups were demonstrated to enhance the interaction of the phthalocyanine molecules with CNTs *via*  $\pi$ -stacking interactions. It was shown that the nature of the mesophases was not altered in these composites and the lateral conductivity of the films tends to increase with the increase of SWCNT concentration as additives, however the sensing properties of such composites obtained by dispersion of small amounts of single-walled carbon nanotubes in liquid crystalline phthalocyanines were not studied at all.

In this work, we studied the dispersion of single-walled carbon nanotubes in liquid crystalline asymmetrically substituted MPc (M=Cu, Co, H<sub>2</sub>) phthalocyanines bearing one pyrene and six polyoxy groups as side chains (Fig. 1). The synthesis of MPc (M=Cu, Co, H<sub>2</sub>) has been published in our previous work [6], however their liquid crystalline properties have not been described so far. LC properties of MPc (M=Cu, Co, H<sub>2</sub>) and the influence of SWCNT on phase behavior of these MPc are

investigated. The structural features and the sensor response of MPc/SWCNT composite thin films to ammonia vapour (10-50 ppm) are studied for the first time and compared with those of the films of pure MPc derivatives.

Fig. 1.

## EXPERIMENTAL

### Synthesis

The synthesis of 2,3,9,10,16,17-hexakis(4,7,10-trioxaundecan-1-sulfanyl)-23(24)-(1-pyrenylmethoxy) metal-free phthalocyanine ( $H_2Pc$ ), 2,3,9,10,16,17-hexakis(4,7,10-trioxaundecan-1-sulfanyl)-23(24)-(1-pyrenylmethoxy) phthalocyaninato copper (II) ( $CuPc$ ) and 2,3,9,10,16,17-hexakis(4,7,10-trioxaundecan-1-sulfanyl)-23(24)-(1-pyrenylmethoxy) phthalocyaninato cobalt(II) ( $CoPc$ ) has already been described elsewhere [6]. MPc/SWCNT dispersion was prepared by adding small amount (1 wt. %) of SWCNT (Sigma-Aldrich) to the phthalocyanine solutions in dichloromethane (Merck) and subjected to sonification for up to 2 h to enhance the nanotubes solubility. Thin films of the obtained composites were deposited by spin coating of their dispersion in dichloromethane onto the substrates for their further investigation.

### Equipment

The phase transition behavior of MPcs was observed using a polarizing optical microscope (POM) (Leitz Wetzler Orthoplan-pol.) equipped with a hot stage (Linkam TMS 93) and a temperature controller (Linkam LNP). Thermogravimetric analysis (TGA) was carried out on a Mettler Toledo Star Thermal Analysis System heated at a rate of  $10\text{ }^\circ\text{C min}^{-1}$  in a nitrogen flow ( $50\text{ mL min}^{-1}$ ). Transition temperatures were determined at a scan rate of  $10\text{ }^\circ\text{C min}^{-1}$  using a Mettler Toledo Star Thermal Analysis System/DSC 822. The differential scanning calorimeter (DSC) system was calibrated with 3 mg indium samples under a nitrogen atmosphere. X-ray diffraction measurements (XRD) ( $\text{Cu-K}_\alpha$ -radiation) were performed using a Bruker Advanced D8 diffractometer.

Optical absorption spectra in the UV-visible region were recorded with Shimadzu UV-Vis-2101 spectrometer. Raman spectra were recorded with a Triplemate, SPEX spectrometer equipped with CCD detector in back-scattering geometry. The 488 nm, 40 mW line of an Ar-laser was used for the spectral excitation.

Scanning electron microscopy (SEM) images were obtained using FEI-nova nanosem 200. Spectroscopic ellipsometry was used to determine the thickness of the films using a Woolam  $M-2000V^{TM}$  rotating analyser spectroscopic ellipsometer in the spectral range of 400-800 nm.

### Sensor properties study

The sensor response to low-concentrations of  $\text{NH}_3$  in the range 10-50 ppm was studied. Pure commercial  $\text{NH}_3$  gas was used as the  $\text{NH}_3$  source, while air was used for dilution and purging of  $\text{NH}_3$  gas. The injection of  $\text{NH}_3$  was carried out at the constant flow of air of 200 mL/min and the exposure time was fixed at 8 s for all films. MPcs and MPc/SWCNT composites were deposited as films by spin casting of their solutions in dichloromethane onto interdigitated Pt electrodes (DropSens, G-IDEPT10). The dimension of gaps is 10  $\mu\text{m}$ ; the number of digits is 125 x 2 with a digit length equal to 6760  $\mu\text{m}$ ; cell constant is  $0.0118\text{ cm}^{-1}$ . Electrical characterization of the films was carried out using a Keithley 236 electrometer by applying a constant dc voltage of 10 V. The thickness of the films as determined by spectral ellipsometry was about 20 nm.

## RESULTS AND DISCUSSION

### Liquid crystalline properties of MPc derivatives and MPc/SWCNT composites

The LC properties of MPcs and their binary mixtures with SWCNT (0.1-1 wt. %) were investigated by POM, thermal gravimetric analysis, DSC, and XRD at room temperature and all these phthalocyanines displayed thermotropic columnar mesomorphism. Liquid crystalline textures typical for columnar discotic mesophases were observed both for MPcs and their composites with SWCNT (1 wt. %) (Fig. 2).

Fig. 2.

No changes of the texture were observed in the temperature range from room temperatures to the temperature of their decomposition. Decomposition temperatures were independently determined by TGA to be 250°C for all studied derivatives.

Figs. 2a, 2c and 2e show typical mosaic textures of pure phthalocyanine derivatives. The textures of the MPc/SWCNT composites (Figs. 2b, 2d, 2f) are noticeably different; inclusion of carbon nanotubes into the columnar matrix leads to an increase of the domains size. It is possible to suggest that SWCNTs dispersed in LC matrix can act as seeds for oriented domain growth as it was observed in the case of nematic liquid crystals [25-27].

In differential scanning calorimeter (DSC) measurements, CoPc, CuPc and H<sub>2</sub>Pc show transitions at about 55°C, 50°C and 49°C for all cooling cycles, respectively. However, no changes in the optical texture are observed on cooling the mesophase between two glass slides under POM, this can be attributed to columnar structure 'frozen' in glassy state [28, 29]. In addition, if the samples were prepared by evaporating a dichloromethane solution of these compounds on one glass slide, a mosaic texture typical for planar alignment was obtained at room temperature without annealing. It can be concluded that CoPc, CuPc and H<sub>2</sub>Pc show columnar structure at room temperature. POM measurements showed that these phthalocyanines transfer to the isotropic liquid state around 250°C with partial decomposition. DSC measurements of the composites with SWCNT (1 wt. %) did not show any significant peak corresponding to any phase transition or to any glassy transition.

Identification of mesophases was performed by XRD measurements and the lattice constant (*a*) was calculated with *d*-spacing and Miller indices,  $hkl$  ( $1/d^2=4/3(h^2 + hk + k^2/a^2)$ ); results are summarised in Table 1. Dichloromethane solutions of CoPc, CuPc, H<sub>2</sub>Pc and their composites were dropped onto glass slides and left for the solvent to evaporate at room temperature. The XRD patterns of the studied samples contained reflections typical of a Col mesophase of substituted phthalocyanines [30]. The four Bragg reflections having reciprocal spacings of  $1:\sqrt{3}:\sqrt{4}:\sqrt{7}$ , which are characteristics of a two-dimensional hexagonal lattice in the columnar mesophase, were observed. According to the low angle region of the XRD pattern, the mesophase could be established as a discotic hexagonal columnar (Col<sub>h</sub>) mesophase. In the wide angle region the compounds show diffused halos at 4.06 Å for CoPc, 4.10 Å for CuPc, 4.13 Å for H<sub>2</sub>Pc and at 4.12 Å, 4.13 Å, 4.18 Å (2θ~20°) for their composites, respectively, which are compatible with the disorder of paraffinic tails in the side chains [31-33].

Table 1.

### Films characterization

The electronic absorption spectra of the solutions and films of H<sub>2</sub>Pc, CoPc and CuPc derivatives before and after heating are given in Fig. 3. Films of the MPc derivatives exhibit optical absorption spectra typical for most metal phthalocyanines

[34]. The maxima of Q-bands attributed to the electron transitions from the HOMO  $a_{1u}$  to LUMO  $e_g$  [34] are located at 657, 650 and 653 nm in the spectra of H<sub>2</sub>Pc, CoPc and CuPc films, respectively.

Fig. 3.

The Q-bands in the spectra of the H<sub>2</sub>Pc, CoPc and CuPc films and their composites with SWCNT are blue shifted relative to the spectra of the corresponding solutions. Such shift of the Q-bands is indicative of the cofacial (face-to-face) arrangement of MPc molecules in the films, which is typical for many phthalocyanines forming Col mesophases [35-36].

The SEM images of the composites (Fig. 4 shows CuPc/SWCNT as an example)) demonstrate that their films have a layered structure consisting of SWCNT nanotube bundles of 10-30 nm in diameter, wrapped by layers of liquid crystalline MPc molecules.

Fig. 4.

The orientation of MPc molecules in the films of MPc derivatives and their composites were studied by polarized Raman spectroscopy. The principles of this method for the investigation of molecular film orientation were described in details in our previous publications [37-38]. This technique resides in estimation of the angle of molecule inclination relative to the substrate surface based on the measurements of the ratio of intensities of the bands for each symmetry type of vibrations in the Raman spectra measured in the parallel ( $I_{ii}$ ) and cross ( $I_{ij}$ ) polarizations of incident and scattering light. The phthalocyanine macrocycle is characterized by  $D_{4h}$  group symmetry where  $A_{1g}$ ,  $B_{1g}$ ,  $B_{2g}$ ,  $E_g$  modes are Raman active. In contrast to the MPcs, the metal-free phthalocyanine (H<sub>2</sub>Pc) molecule is of  $D_{2h}$  symmetry. Therefore, in the present case the tilt angle should be estimated using the polarizability tensor for  $D_{2h}$  point group. However, this would introduce a third tensor element due to the additional twist between the benzene rings. Thus, we assumed that the polarizabilities of the H<sub>2</sub>Pc in x and y directions are the same. In other words, to simplify the calculations of the tilt angles, we treated the H<sub>2</sub>Pc as a molecule of  $D_{4h}$  symmetry.

The nonpolarized Raman spectra of MPc films are given in Fig. 5a. The Raman spectra of films of the CuPc derivative and its composite deposited on glass substrates in parallel ( $ii$ ) and cross ( $ij$ ) polarizations are shown in Fig. 5b as an example. The intensities of the strongest lines with known symmetry types were measured (Fig. 5b). It has already been shown that there are no intensive bands belonging to organic substituents in the range from 300 to 1650  $cm^{-1}$  in the Raman spectra of substituted phthalocyanines due to the resonance character of the Raman spectra excited by the lasers of visible region [39].

Fig. 5.

The average values of  $I_{ii}/I_{ij}$  were 3.7, 3.6 and 1.4 for  $A_{1g}$ ,  $B_{1g}$  and  $B_{2g}$  modes in the Raman spectra of CuPc films, while in the case of the films of CuPc/SWCNT-1% composite these values were 3.9, 3.2 and 1.4. The angles of inclination of molecules relative to the substrate surface in the films of CuPc and CuPc/SWCNT-1% were calculated to be 85° and 82°, respectively. Similar data were also obtained for H<sub>2</sub>Pc, CoPc and their composites. Therefore, inclusion of carbon nanotubes into the columnar matrix of the MPcs does not lead to the change of LC properties of the investigated materials and the orientation of their films. As most of LC phthalocyanines the films of H<sub>2</sub>Pc, CoPc, CuPc and their composites with SWCNT have planar alignment [10].

### Sensor response of MPc and MPc/SWCNT composite films to ammonia

The sensor properties of thin films' of MPc and MPc/SWCNT composites containing different amounts of SWCNT toward NH<sub>3</sub> (10-50 ppm) were studied using chemiresistive method. The typical sensor responses  $R_n$  ( $R_n = (R - R_0)/R_0$ ,

where  $R_0$  is the resistance value at the beginning of an exposure/recovery cycle and  $R$  is the resistance of the film at a certain  $\text{NH}_3$  concentration) of the MPc films are shown in Fig. 6. All three derivatives exhibit strong and reversible sensor response to ammonia (10-50 ppm).

Fig. 6.

The sensor response value increases in the order  $\text{H}_2\text{Pc} < \text{CuPc} < \text{CoPc}$ . This order is in good agreement with the results obtained by Liang et al. [40] showing by the first-principle density functional theory that the central metals play a critical role in the sensitivity towards  $\text{NH}_3$ . To study the effect of incorporation of SWCNT into phthalocyanine matrix, the sensor response of the composites containing different amounts of carbon nanotubes was measured.  $R_n$  of CoPc/SWCNT containing 0.1, 0.5, 0.75 and 1 wt. % SWCNT is given in Fig. 7 as an example. The dependence of the  $R_n$  on ammonia concentration for MPc/SWCNT-1% (M=2H, Cu, Co) is given in Fig. 8 in order to compare the effect of the central metal in the phthalocyanine macrocycle on the sensor response.

Fig. 7.

Fig. 8.

The sensor response value increases in the order  $\text{H}_2\text{Pc/SWCNT} < \text{CuPc/SWCNT} < \text{CoPc/SWCNT}$  which is similar to the case of pure MPc films.

It is worth mentioning that the film resistance decreases from  $10^7$ - $10^8 \Omega \cdot \text{m}$  to about  $10^5 \Omega \cdot \text{m}$  with the addition of 1 wt. % of SWCNT. The increase of films conductivity makes it possible to use simple equipment for the conductivity measurements and does not require the employment of expensive electrometers for precision high resistance and low current measurements. However it is necessary to mention that the addition of SWCNT leads to the decrease of the relative sensor response of the composites compared to that of pure phthalocyanine films. Fig. 7 shows that the more amount of SWCNT incorporated into the matrix of LC phthalocyanine the less relative sensor response to ammonia is observed.

## CONCLUSIONS

The dispersion of single-walled carbon nanotubes in liquid crystalline asymmetrically substituted phthalocyanines MPc (M=Cu, Co, 2H) bearing one pyrene and six polyoxy groups as side chains was studied and their composite films were examined for ammonia detection. The influence of SWCNT on phase behavior of MPcs was investigated by XRD, polarized optical microscopy and differential scanning calorimetry. It was demonstrated that the incorporation of small amounts of SWCNT (0.1-1 wt. %) does not alter the MPc mesophases nor does it change the orientation of their films. Both MPc derivatives and their composites with carbon nanotubes form  $\text{Col}_h$  mesophases at room temperature. The chemiresistive sensor response of MPc/SWCNT composite thin films to ammonia vapour (10-50 ppm) were studied and compared with those of the films of pure MPc derivatives. The sensor response to ammonia of both MPc films and composite films increases in the order  $\text{H}_2\text{Pc} < \text{CuPc} < \text{CoPc}$ . On the one hand, the film resistance decreases from  $10^7$ - $10^8 \Omega \cdot \text{m}$  to about  $10^5 \Omega \cdot \text{m}$  with the addition of 1 wt. % of SWCNT, which makes it easier for the measurements without the need of expensive electrometers for precision high resistance measurements. On the other hand, the addition of SWCNT leads to a decrease of the relative sensor response of the composites compared to that of pure phthalocyanine films.

## Acknowledgements

This work was supported by the Scientific and Technological Research Council of Turkey (TUBITAK, Project number: 111M699) and the basic project of the Nikolaev Institute of Inorganic Chemistry SB RAS.

## REFERENCES

1. Bottari G, Suanzes JA, Trukhina O and Torres T. *J. Phys. Chem. Lett.* 2011; **2**: 905–913.
2. Jurow M, Schuckman AE, Batteas JD. and Drain CM. *Coord. Chem. Rev.* 2010; **254**: 2297–2310.
3. Kamei T, Kato T, Itoh E and Ohta K. *J. Porphyrins Phthalocyanines* 2012; **16**: 1261–1275.
4. Frischmann PD, Mahata K and Wurthner F. *Chem. Soc. Rev.* 2013; **42**: 1847–1870.
5. Kaya EN., Tuncel S, Basova TV, Banimuslem H, Hassan A, Gürek AG, Ahsen V, Durmuş M. *Sensors Actuators B* 2014; **199**: 277–283.
6. Kaya EN., Basova T, Polyakov M, Durmuş M, Kadem B, Hassan A. *RSC Advances* 2015; **5**: 91855–91862.
7. Gülmez AD., Polyakov MS, Volchek VV, Kostakoğlu ST, Esenpinar AA, Basova TV, Durmuş M, Gürek AG, Ahsen V, Banimuslem H, Hassan A. *Sensors Actuators B* 2017; **241**: 364–375.
8. Kiliç N, Öztürk S, Atilla D, Gürek AG, Ahsen V, Öztürk ZZ. *Sensors and Actuators B* 2012; **173**: 203–210.
9. Shi J, Luan L., Fang W, Zhao T, Liu W, Cui D. *Sensors Actuators B* 2004; **204**: 218–223.
10. Basova T, Hassan A, Durmuş M, Gürek AG, Ahsen V. *Coord. Chem. Rev.* 2016; **310**: 131–153.
11. Sergeev S, Pisula W, Geerts YH. *Chem. Soc. Rev.* 2007; **36**: 1902–1929.
12. Jha P, Sharma M, Chouksey A, Chaturvedi P, Kumar D, Upadhyaya G, Rawat JSBS, Chaudhury PK. *Synth. React. Inorg. Metal–Org. Nano-Metal Chem.* 2014; **44**: 1551–1557.
13. Mugadza T, Nyokong T. *J. Coll. Interface Sci.* 2011; **354**: 437–447.
14. Wang Y, Hu N, Zhou Z, Xu D, Wang Z, Yang Z, Wei H, Kong ES-W, Zhang Y. *J. Mater. Chem.* 2011; **21**: 3779–3787.
15. Tuncel S, Kaya EN, Durmuş M, Basova T, Gürek AG, Ahsen V, Banimuslem H, Hassan A. *Dalton Transactions* 2014; **43**: 4689–4699.
16. Mugadza T and Nyokong T. *Polyhedron* 2011; **30**: 1820–1829.
17. Ogbodu RO, Antunes E and Nyokong T. *Dalton Transactions* 2013; **42**: 10769–10777.
18. Wang B, Zhou X, Wu Y, Chen Z, He C. *Sensors and Actuators B* 2012; **171-172**: 398–404.
19. Wang B, Wu Y, Wang X, Chen Z, He C. *Sensors and Actuators B* 2014; **190**: 157–164.
20. Lucci M, Reale A, Carlo DA, Orlanducci S, Tamburri E, Terranova ML, Davolic I, Di Natale C, D’Amico A, Paolesse R. *Sensors and Actuators B* 2006; **118**: 226–231.
21. Alwarappan S, Liu G, Li CZ. *Nanomedicine: Nanotechnol., Biology Medicine*, 2010; **6**: 52–57.
22. Jyothirmayee Aravind SS and Ramaprabhu S. *Sensors and Actuators B* 2011; **155**: 679–686.
23. Polyakov MS, Basova TV, Göksel M, Şenocak A, Demirbaş E, Durmuş M, Kadem B, Hassan A. *Synth. Met.* 2017; **227**: 78–86.
24. Jurow M, Varotto A, Manichev V, Travlou NA, Giannakoudakis DA, Drain CM. *RSC Adv.* 2013; **3**: 21360–21364.
25. Russell JM, Oh S, LaRue I, Zhou O and Samulski ET. *Thin Solid Films* 2006; **509**: 53–57.

26. Dierking I, Scalia G, Morales P and LeClere D. *Adv. Mater.* 2004; **16**: 865–869.
27. Mrozek RA., Kim B, Holmberg VC and Taton TA. *Nano Lett.* 2003; **3**: 1665–1669.
28. Brewis M, Clarkson GJ., Holder AM. and McKeown NB. *Chem. Commun.* 1998; 969–970.
29. Treacher KE, Clarkson GJ, McKeown NB. *Liquid Crystal* 1995; **19**: 887–889.
30. Simon BP. J, *Phthalocyanine based liquid crystals: towards submicronic devices*, vol. 2. Leznoff CC, Lever ABP, editors. Phthalocyanines: properties and applications. New York: VCH, 1993; 223–299.
31. Dabak S, Ahsen V, Heinemann F, Zugenmaier P. *Mol. Cryst. Liq. Cryst.* 2000; **348**: 111–127.
32. Basova T, Kol'tsov E, Gürek AG, Atilla D, Ahsen V, Hassan AK. *Mater. Sci. Eng. C Biomim. Supramol. Syst.* 2008; **28**: 303–308.
33. Gürek AG, Durmuş M, Ahsen V. *New J. Chem.* 2004; **28**: 693–699.
34. Ishi K, Kobayashi N. *The Photophysical Properties of Phthalocyanines and Related Compounds*, vol. 16. K.M. Kadish, K.M. Smith, R. Guillard (Eds.), The porphyrin Handbook, Academic Press, 1999; 1–42.
35. Basova TV, Çamur M, Esenpınar AA, Tuncel S, Hassan A, Alexeyev A, Banimuslem H, Durmuş M, Gürek AG, Ahsen V. *Synth. Met.* 2012; **162**: 735–742.
36. Hatsusaka K, Ohta K, Yamamoto I, Shirai H. *J. Mater. Chem.* 2001; **11**: 423–433.
37. Basova TV, Kiselev VG, Plyashkevich VA, Cheblakov PB, Latteyer F, Peisert H, Chassè T. *Chem. Phys.* 2011; **380**: 40–47.
38. Basova TV, Durmuş M, Gürek AG, Ahsen V, Hassan A. *J. Phys. Chem. C* 2009; **113**: 19251–19257.
39. Basova TV, Kolesov BA, Gürek AG and Ahsen V. *Thin Solid Films* 2001; **385**: 246–251.
40. Liang X, Chen Z, Wu H, Guo L, He C, Wang B and Wu Y. *Carbon* 2014; **80**: 268–278.

Fig. 1. Structure of asymmetrical type phthalocyanine compounds MPc, where M = 2H, Cu or Co.

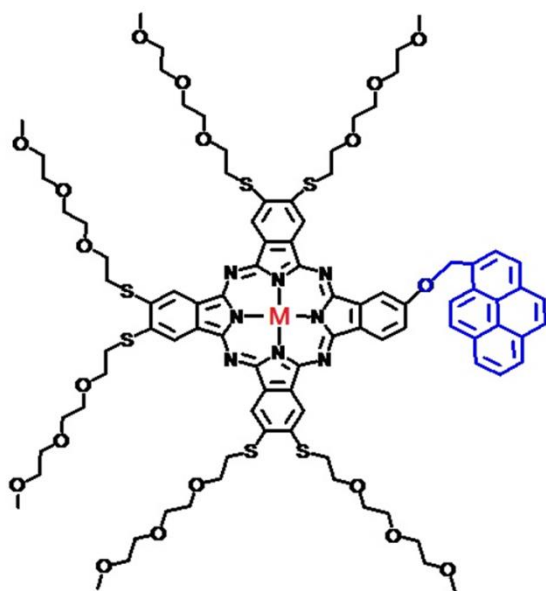


**Fig. 2.** Polarized optical microscopy images of metal phthalocyanines (CoPc (a), CuPc (c) and H<sub>2</sub>Pc (e)) and their composites (CoPc/SWCNT-1% (b), CuPc/SWCNT-1% (d) and H<sub>2</sub>Pc/SWCNT-1% (f)).

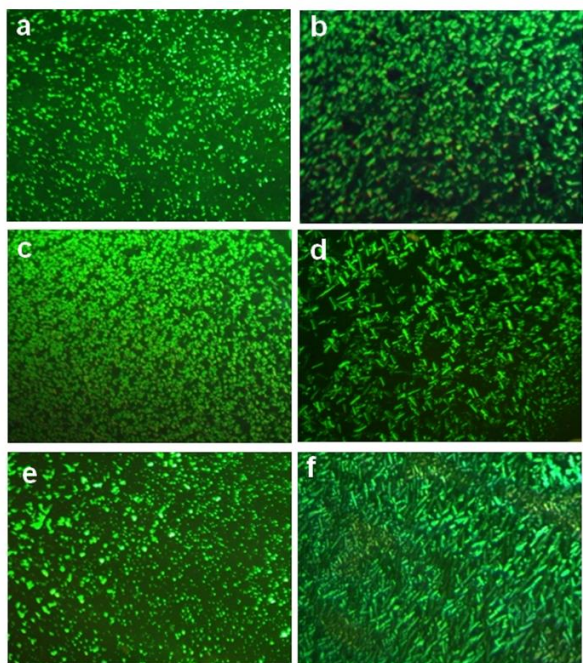


**Fig. 3.** Optical absorption spectra of solutions (a, black curves) and films of H<sub>2</sub>Pc, CoPc and CuPc derivatives (b, blue lines) as well as their hybrids containing 1% (c, red lines) of SWCNT.

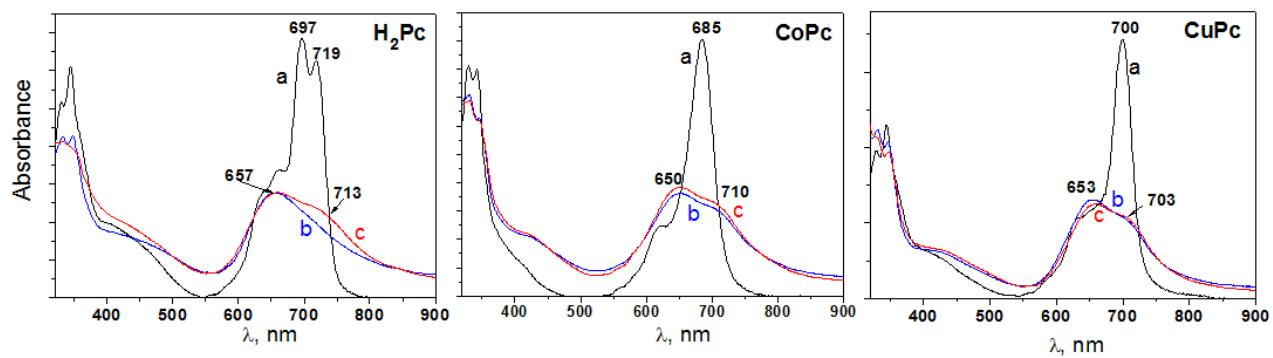


**Fig. 4.** SEM image (edge view) of CuPc/SWCNT-1% film.

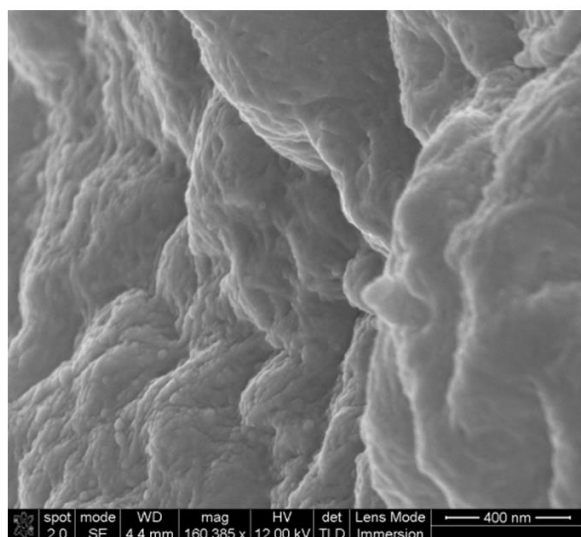


**Figure 5.** Raman spectra of H<sub>2</sub>Pc, CuPc and CoPc derivatives (a); polarized Raman spectra of CuPc and CuPc/SWCNT-1% films, measured in parallel (ii) and cross (ij) polarizations of incident and scattering light (b). The Raman bands labelled with an asterisk correspond to those overlapped with SWCNT modes.

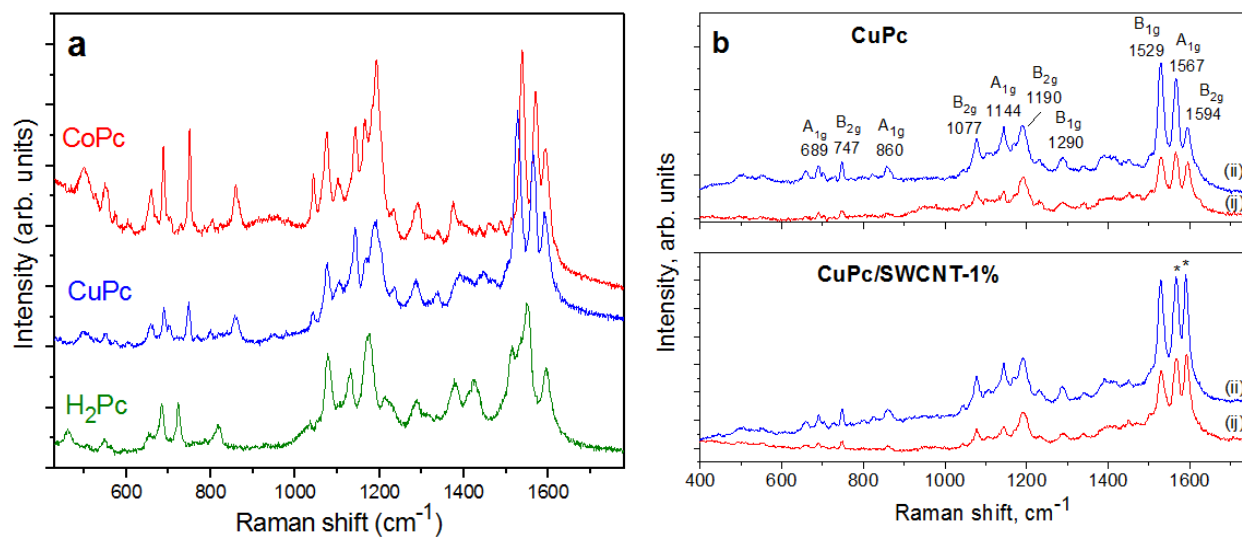
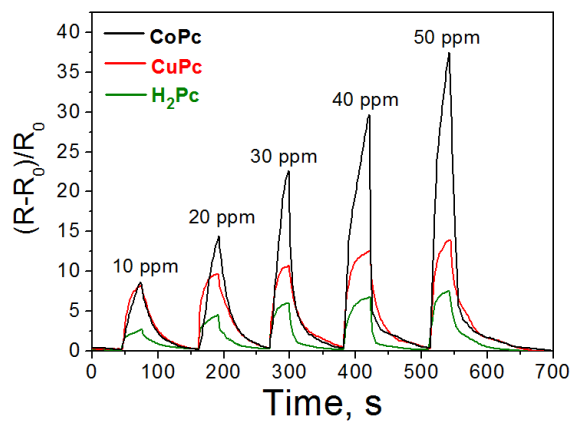


Fig. 6. Sensor response of MPc films (M=Co, Cu, 2H) towards ammonia (10-50 ppm).



**Fig. 7.** Typical sensor response of thin films of CoPc/SWCNT containing 0.1, 0.5, 0.75 and 1 wt. % SWCNT towards ammonia (10, 30 and 50 ppm).

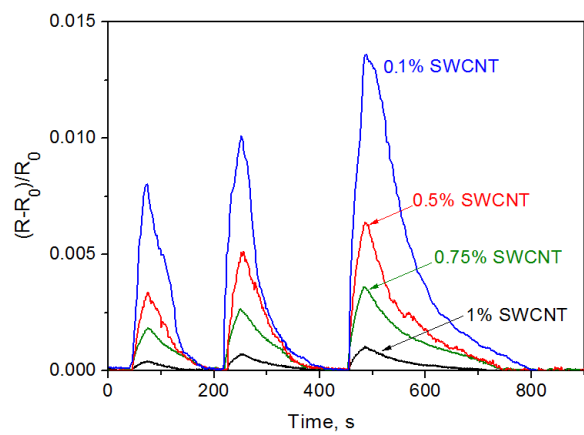
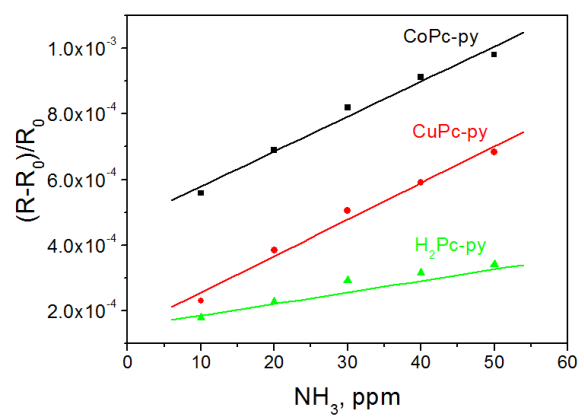


Fig. 8. Response of MPc/SWCNT-1% hybrid films towards NH<sub>3</sub> concentrations.



**Table 1.** XRD data of the studied metal phthalocyanines CoPc, CuPc, H<sub>2</sub>Pc and their composites CoPc/SWCNT-1% , CuPc/SWCNT-1% and H<sub>2</sub>Pc/SWCNT-1% at room temperature.

Compound	Phase	Observed spacings (Å)	Calculated spacings (Å)	Lattice parameters (Å)	Miller indices (hkl)
<b>CuPc</b>	Col <sub>h</sub>	21.02	21.02	24.27	100
		12.10	12.13		110
		10.49	10.51		200
		8.01	7.94		210
<b>CuPc/SWCNT-1%</b>	Col <sub>h</sub>	21.61	21.61	24.95	100
		12.9	12.48		110
		10.72	10.80		200
		8.25	8.17		210
<b>CoPc</b>	Col <sub>h</sub>	21.65	21.65	24.99	100
		13.46	12.50		110
		10.84	10.82		200
		8.84	8.18		210
<b>CoPc/SWCNT-1%</b>	Col <sub>h</sub>	21.81	21.81	25.18	100
		13.46	12.59		110
		11.76	10.90		200
		8.92	8.24		210
<b>H<sub>2</sub>Pc</b>	Col <sub>h</sub>	21.87	21.87	25.25	100
		12.41	12.62		110
		10.18	10.93		200
		8.38	8.26		210
<b>H<sub>2</sub>Pc/SWCNT-1%</b>	Col <sub>h</sub>	21.73	21.73	25.09	100
		12.24	12.54		110
		10.63	10.84		200
		9.33	8.21		210